Available online at www.sciencedirect.com
SCIENCE DIRECT®
Journal of Theoretical Biology 226 (2004) 169–175
Journal of Theoretical Biology
www.elsevier.com/locate/jtbi

A kinetic model of telomere shortening in infants and adults

Igor A. Sidorov*, Dennis Gee, Dimiter S. Dimitrov

NCI-Frederick, NIH, Bldg. 469/Rm. 110, P.O. Box B, Frederick, MD 21702-1201, USA

Received 12 May 2003; received in revised form 31 July 2003; accepted 19 August 2003

Abstract

We have previously demonstrated that telomeres shorten more rapidly in peripheral mononuclear cells (PBMC) of infants than in adults (Zeichner et al., Blood 93 (1999) 2824). Here we describe a mathematical model that allows quantification of telomere dynamics both in infants and in adults. In this model the dependence of the telomere dynamics on age is accounted by assuming proportionality between the body growth, as approximated by the Gompertz equation, and the increase in the number of PBMCs. The model also assumes the existence of two subpopulations of PBMC with significantly different rates of division. This assumption is based on the results from a previous analysis of in vitro data for telomere dynamics in presence of telomerase inhibitors and our recent data obtained by measurements of BrdU incorporation in T lymphocytes in humans (Kovacs et al., J. Exp. Med. 194 (2001) 1731). The average telomere length of PBMC was calculated as the average length of these two subpopulations. The model fitted our experimental data well and allowed to derive a characteristic time of conversion of the rapidly proliferating cells to slowly proliferating cells on the order of 20 days. The half-life of the slowly proliferating cells was estimated to be about 6 months, which is in good agreement with data obtained by independent methodologies. Comparison of the one-population and two-subpopulations models demonstrated that one population model cannot explain the observed parameters of the terminal restriction fragment (TRF) dynamics while two-subpopulations model does. These results suggest that the rapid telomere shortening in infants is largely determined by the faster PBMC turnover compared to adults. This may have major implications for elucidation of the HIV pathogenesis in infants. One can speculate that the more rapid course of the HIV disease in infants is due to the existence of rapidly dividing cells, which are susceptible to HIV infection. In addition, these results could have implications for understanding of mechanisms of aging.

Keywords: Telomere dynamics; Aging; Kinetic model

1. Introduction

DNA-protein complexes at the chromosome termini (telomeres) play a major role in chromosome stability. Telomeric DNA sequences are lost after each cell division if not restored by the ribonucleoprotein enzyme telomerase (Allsopp et al., 1992; Blackburn, 1991). Therefore, the telomere length can be used as a marker of the total number of cell divisions and hence as a correlate of the aging process (Greider, 1996).

Telomerase is expressed during embriogenesis in humans. It was found in (Ulaner and Giudice, 1997) that all examined tissues (liver, lung, spleen, testis, kidney, brain, and heart) expressed telomerase activity at the earliest stage analysed. This activity was not detected in the somatic tissues examined from the neonatal period onward (Wright et al., 1996). Immune system undergoes dramatic developmental changes during infancy (Wilson et al., 1996). For an *in vivo* system of low or absent telomerase activity telomere lengths of PBMC shorten more rapidly in infants then in adults (four-fold difference (Zeichner et al., 1999)). One of possible explanations of this phenomenon is the existence of two (or more) cell subpopulations with different rates of telomere shortening. We have also hypothesized that: (1) changes in the rate of growth for PBMC are correlated with a decrease in body growth; (2) both subpopulations have a non-zero rate of cell turnover; and (3) the proportion between growing and non-growing subpopulation is constant.

Using these assumptions, we propose a model that describes the dynamics of telomere lengths in the two

*Corresponding author. Tel.: +1-301-846-1449; fax: +1-301-846-6189.
E-mail address: sidorovi@ncifcrf.gov (I.A. Sidorov).

0022-5193/$ - see front matter © 2003 Elsevier Ltd. All rights reserved.
doi:10.1016/j.jtbi.2003.08.009

cell subpopulations. Experimental data derived for infants and adults (Feng et al., 1999; Zeichner et al., 1999) were fitted to the model solution. Parameter values after fitting have biologically reasonable values. The results suggest that the rapid telomere shortening in infants is largely determined by the faster PBMC turnover compared to adults.

2. Methods

2.1. Telomere length measurements

Telomere length measurements in samples from children and adults were performed as previously described (Zeichner et al., 1999). Data were processed as described below (see next section). Mean and standard deviation were calculated for each time point.

2.2. Terminal restriction fragment (TRF) lengths distribution

Measurements based on Southern blots were used for the quantitative analysis of TRF lengths distribution. Gel images were digitized using Bio-Rad Molecular Analyst (Ver. 1.5) at resolution (r) either 0.1 or 0.2 mm. Pairs of data points (D_i, S_i), $i = 1, \ldots, N$ were obtained for each lane, where: D_i, DNA migration distance on the blot (mm); S_i, average signal intensity (AU). The values of D_i were chosen so that the inequality $D_i < D_{i+1}$ holds and the difference $D_{i+1} - D_i = r$ was constant for $i = 1, \ldots, N-1$. Average signal intensity was calculated as $S_i = (S_i^1 + S_i^2 + \cdots + S_i^k)/k$, where k is the number of pixels across the lane. Background signal intensity depended linearly on migration distance $S_0 = S_0^A + DS_0^B$ and it was accounted by subtracting from all the measurements: $S_i \equiv S_i - S_0$. Parameters S_0^A, S_0^B were calculated by fitting the data to normal probability distribution function with linear background.

Each TRF consists of telomeric and subtelomeric sequence (Harley, 1997). For TRFs hybridized to the labeled telomeric probe $[^{32}P](TTAGGG)_n$ the intensity corresponding to one molecule of TRF is equal to $\alpha\hat{L}S_p$ where: $\hat{L}$, telomere length; S_p, intensity of one probe molecule; and α, coefficient.

The values of D_i, S_i for $i = 1, \ldots, N$ can be considered as $S_i \equiv S_i^1 + S_i^2 + \cdots + S_i^{N_i}$, where intensity S_i^j corresponds to migration distance D_i^j and $D_i - r/2 \leqslant D_i^j < D_i + r/2$. Here: N_i is the number of TRF molecules having intensity S_i^j and migration distance D_i^j, $j = 1, \ldots, N_i$. Let us assume for simplicity that $S_i^1 = S_i^2 = \cdots = S_i^{N_i} = \hat{S}_i$ and, therefore, $S_i = N_i\hat{S}_i = \alpha S_p N_i \hat{L}_i$, where: $\hat{L}_i = L_i - L_T$, telomere length; L_i, length of TRF; and L_T, subtelomeric sequence length. Because of $D_{i+1} - D_i = r$ for all $i = 1, \ldots, N-1$, the values

$$\frac{rN_i}{\sum_{i=1}^N rN_i} = \frac{S_i}{(L_i - L_T)\sum_{i=1}^N S_i/(L_i - L_T)}, \quad i = 1, \ldots, N$$

can be considered as frequency values of TRF migration distance distribution.

The dependence of the natural logarithm of the TRF length on migration distance was quasi-linear for our experimental data and the polynomial, $\ln(L) = a_0 + a_1 D + a_2 D^2 + a_3 D^3$, was used to describe this dependence. Parameter values (a_0, a_1, a_2, a_3) were found by fitting the marker lane data (usually about 5–7 values of marker molecular weights and distances) to the polynomial.

Let the probability density function f_D characterize the distribution of migration distance D. If the dependence of TRF length on migration distance $L = L(D)$ is known and the inverse function $D = D(L)$ exists, then

$$P(L(D_1) < L \leqslant L(D_2)) = \int_{L(D_1)}^{L(D_2)} \frac{\mathrm{d}D(L)}{\mathrm{d}L} f_D(D(L))\,\mathrm{d}L,$$

where $P(\cdot)$ is the probability. It follows from this formula that if TRF migration distances have normal distribution and logarithm of TRF length depends linearly on migration distance then the resulting distribution of TRF lengths will be lognormal. Values of the function $D(L)$ can be found as a solution (one real root) of the equation $a_0 + a_1 D + a_2 D^2 + a_3 D^3 - \ln(L) = 0$ for given L. Using the discrete representation of f_D and the dependence $D = D(L)$, one can calculate the histogram characterizing the TRF lengths distribution.

2.3. Models of cell and telomere dynamics

2.3.1. One-population model

To describe the cell and telomere dynamics we used the exponential model of tumor growth (see (Sidorov et al., 2003) for details) along with the terms relating to the inhibition of growth. In this model cells can divide with the rate a and population increases in volume proportional to the number of cells. With each cell division the telomere length decreases by l until reaching a critical length L_c. Then the cells die with a constant rate d. Differential equations describing the kinetics of growth are

$$\frac{\mathrm{d}V}{\mathrm{d}t} = \begin{cases} (a-f)V, & L > L_c, \\ -\mathrm{d}V, & L \leqslant L_c, \end{cases}$$

where f corresponds to the different models ($=0$, bV, or $b\ln V$, for exponential, logistic and Gompertz model, respectively); and b, constant which relates to the factors inhibiting tumor growth. The model assumes that cell loss during uninhibited cell growth is accounted by the constant b in the logistic and Gompertz model and cells

die with a rate dV after their telomeres reach the critical length.

Telomere length L for cell population is calculated as $L = \max(L_c, L^0 - nl)$, where L^0 is the initial telomere length. The number of cell divisions n is calculated assuming that the deviation of the population dynamics from the exponential growth is not due to cell death but rather to slowing down the cell division. Therefore,

$$n = \begin{cases} \ln(V/V^0)/\ln 2, & L > L_c, \\ (L^0 - L_c)/l, & L \leqslant L_c, \end{cases}$$

where V^0 is volume of cells at $t = 0$.

For the Gompertz model the expression for n is $n = (a - b \ln V_0)(1 - e^{-bt})/(b \ln 2)$ (Swan, 1987). When $b = 0$ this equation can be reduced to $n = at/\ln 2$, which corresponds to the exponential growth model.

2.3.2. Two subpopulations model: dynamics of growing and non-growing fractions

Let us assume now (as in Sidorov et al., 2002) that cells grow exponentially ($f = 0$) and the whole population is divided on growing and non-growing fractions $V = V^+ + V^-$ with telomere lengths L^+ and L^-, respectively. Let us assume also that cells in the growing fraction can convert to a non-growing state with rate constant q (we will consider below time interval where $L^+ > L_c$ so the equation describing the cells death can be omitted). Thus,

$$\frac{dV^+}{dt} = (a - q)V^+,$$

$$\frac{dV^-}{dt} = qV^+.$$

Let us assume also that for any time t (including $t = 0$) the ratio δ between growing and non-growing fraction of cells is constant, so $V^+/V = 1 - V^-/V = \delta$. In this case the following equation must hold: $q = a(1 - \delta)$.

To compensate the decreased rate of population growth (only growing cells can increase the population size) the parameter value of exponential growth have to be changed as: $\hat{a} = a/\delta$. The rate of cell conversion to the non-growing subpopulation has to be calculated in this case using the formula $\hat{q} = \hat{a}(1 - \delta)$. This relation between the parameters can provide the exponential growth of the whole population with rate a when only δ fraction (constant value) of cells can grow.

The dynamics of L^+ can be calculated as $L^+ = \max(L^0 - lat/\ln 2, L_c)$ taking into account only the growth rate coefficient a. For the non-growing fraction it was assumed that the mean telomere length is determined by the decreasing telomere length of cells from the growing fraction passing to non-growing state with time:

$$\frac{dL^-}{dt} = (L^+ - L^-)\frac{qV^+}{V^-}.$$

For simplicity we assumed that initial conditions for both fractions are the same: $L^+(0) = L^-(0) = L^0$.

Let us assume now that the growth and accumulation of non-growing fraction follows the Gompertz-like model of cell dynamics:

$$\frac{dV^+}{dt} = (a - q)V^+ - bV^+ \ln(V^+ + V^-),$$

$$\frac{dV^-}{dt} = qV^+ - bV^- \ln(V^+ + V^-).$$

If $V^+ = \delta V$ $(0 < \delta \leqslant 1)$ for all t then the dynamics of growing fraction can be calculated as

$$\frac{dV^+}{dt} = (a + b \ln \delta - q)V^+ - bV^+ \ln V^+$$

and, therefore, the equation for telomere loss with time is

$$L^+ = L^0 - (a + b \ln \delta - b \ln V_0^+)\frac{1 - e^{-bt}}{b \ln 2} l,$$

taking into account only the growth rate coefficient $a + b \ln \delta$ and assuming again that the deviation from the exponential growth is due to suppression of cell division and lead to an increase in population doubling time. The telomere length dynamics for non-growing cells is the same as shown above (see equation for dL^-/dt).

It was assumed also that there is a non-zero rate of turnover (u) for both subpopulations. Introduction of this non-zero cell turnover for both growing and non-growing cell subpopulations led to the following equation for telomere length dynamics:

$$L^+ = L^0 - (a + b \ln \delta - b \ln V^0)\frac{1 - e^{-bt}}{b \ln 2} l - ult/\ln 2,$$

$$\frac{dL^-}{dt} = (L^+ - L^-)\frac{qV^+}{V^-} - ul/\ln 2.$$

For the equations describing the dynamics of cells subpopulations (growing and non-growing) it corresponded to the term $uV^\pm - uV^\pm = 0$ on the right-hand side of these equations and did not change cell dynamics. The average value of telomere length for total cell population was calculated using the formula:

$$L = \frac{L^+V^+ + L^-V^-}{V^+ + V^-}.$$

One-population model can be obtained from two-subpopulations model when $\delta = 1$.

2.3.3. Model solutions and data fitting

The solution of the initial-value problem for all differential equation was performed using the DIFSUB_DDE code as previously described (Marchuk et al., 1991). The nonlinear least squares method was used to fit the model solution to experimental data.

3. Results and discussion

We showed previously that telomerase activity in PBMC from infants was undetectable (Zeichner et al., 1999) and therefore one can assume that their cells divided under conditions of negligible telomerase activity. Southern blot images of longitudinal (3 to 36 months) PBMC samples from one patient and mean TRF length are shown in Fig. 1A. One can see that the mean TRF length decreases with time. To calculate the histogram values for each PBMC sample the nonlinear effects in gels as well as linear dependence of background signal intensity on migration distance were taken into account. The histogram in Fig. 1B shows that TRF lengths distribution is changed also with age. Number of cells having TRF lengths from 12.3 to 22.3 kb decreases for the with time and increase for the interval from 5.6 to 9.0 kb.

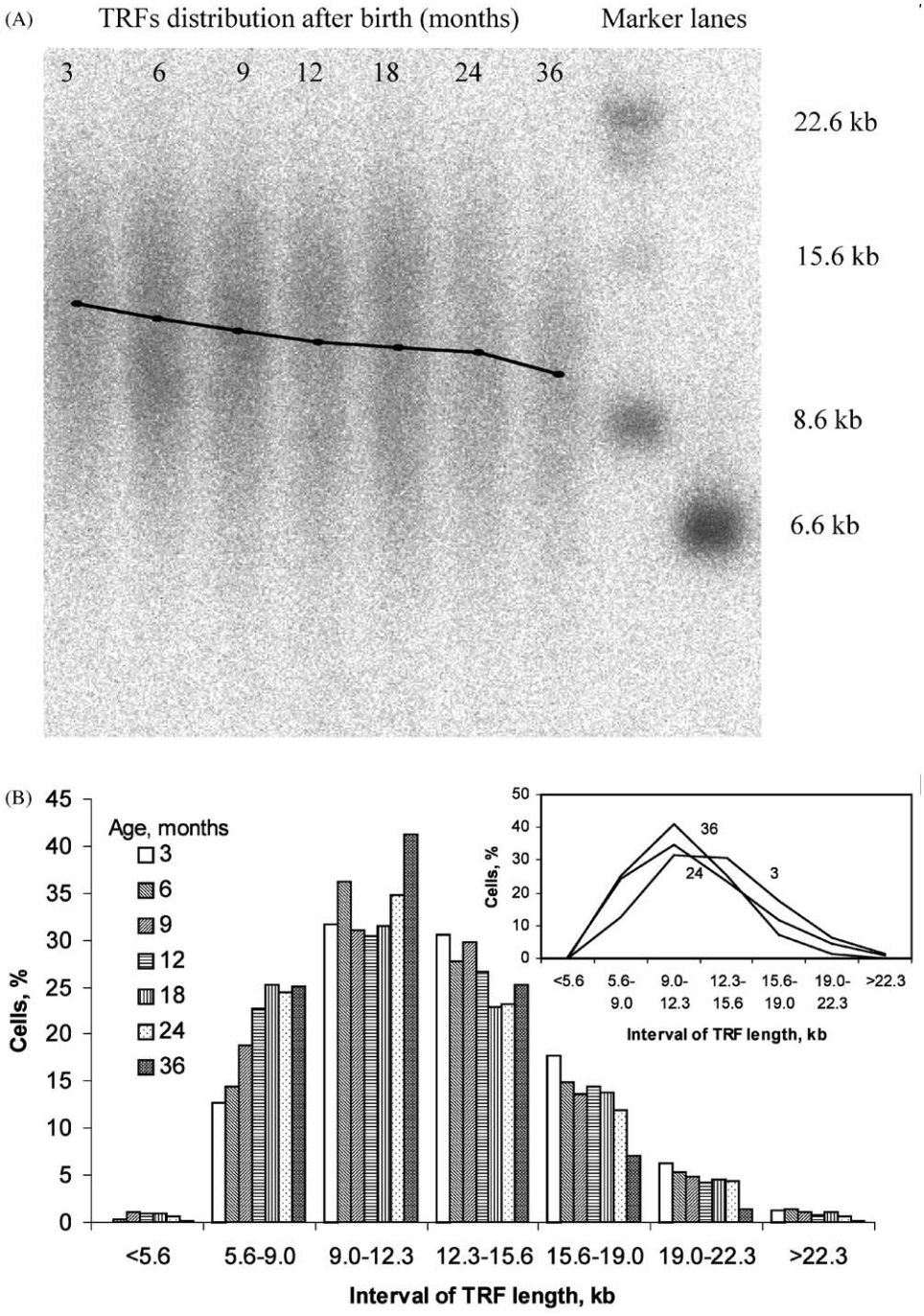

Fig. 1. (A) Southern blot analysis of TRF migration distance distribution for an infant aged from 3 to 36 months. Calculated values of mean TRF length for each sample are shown (●, ——). (B) Dependence of TRF lengths distribution of PBMC on time for this patient. The insert shows TRF lengths distribution for different times after birth.

To analyse the dependence of the TRF distribution on age and evaluate cell dynamics in the absence of telomerase activity we used the one- and two-subpopulation models described above. First, Gompertz model of body growth $dV/dt = V(a - b \ln V)$ was fitted to the dynamics of man growth (age, years/body weight, kg): $V = 0/3.5$, $0.5/7.5$, $1/10$, $2/14$, $3/16$, and $25/70$. Based on the fitting the following parameters of growth were derived: rate of exponential growth $a = 1.122\,\text{year}^{-1}$ and the rate of growth inhibition $b = 0.264\,\text{year}^{-1}$. It was assumed that the PBMC volume in man is proportional to the body weight and the inhibition of PBMC growth is equal to the inhibition of body growth, so parameters a and b were used for the description of PBMC dynamics. Here again it was assumed that deviation of the body dynamics from the exponential growth is due to slowing down the cell division.

Fig. 2 represents the results of fitting the one- and two-subpopulation models to the data. Parameter values are shown in the Table 1. The same values of parameters describing body weight dynamics were used for both models.

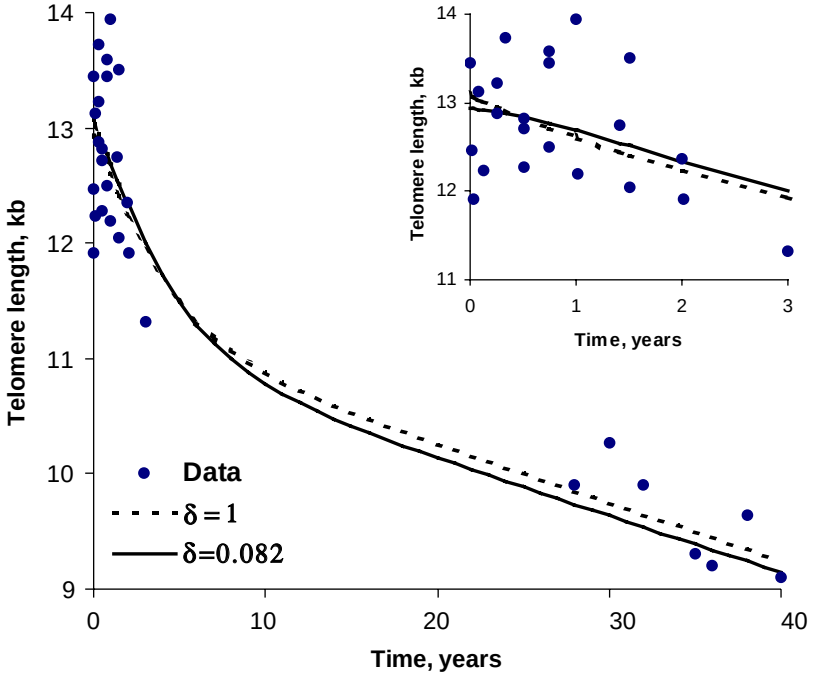

Fig. 2. Telomere loss with age: •, experimental data for four children and two adults; ——, - - - -, theoretical curves for one- ($\delta = 1$) and two-subpopulations model ($\delta = 0.082$), respectively. Gompertz model with dividing of cell population on growing and non-growing fractions was used for simulations. Parameter values are shown in Table 1. Insert shows telomere length dynamics in interval 0–3 years.

Table 1
Parameter values after data fitting for one- and two-subpopulations models

Parameters		Dimension	One-subpopulation	Two-subpopulations
Body weight dynamics				
	a	year^{-1}	1.122	1.122
	b	year^{-1}	0.264	0.264
	V^0	kg	3.5	3.5
Cell and telomere length dynamics				
	L^0	kb	13.08	12.93
	δ	—	1.0[a]	0.082
	u	year^{-1}	0.082	1.36
	l	kb/division	0.423	0.025[a]
Dependent parameters				
	$\hat{a} = a/\delta$	year^{-1}	1.122	13.7
	$\hat{q} = \hat{a}(1 - \delta)$	year^{-1}	0.0	12.6

[a] Fixed value during the fitting.

While one-subpopulation model showed good quality of fitting the value of parameter characterizing the telomere shortening with each cell division was unlikely large: $l = 0.423$ kb/division (the range of l can be estimated as 0.015–0.100 kb/division (Allsopp et al., 1992; Harley et al., 1990; Shammas et al., 1999; Weng et al., 1995; Zhang et al., 1999)).

Two-subpopulation model showed also good fitting to the telomere dynamics (Fig. 2, value of parameter l was fixed at 0.025 kb/division). This model suggests the existence of at least two cell subpopulations with half-life of about 20 days and 6 months, respectively. The TRF length L_0 at time zero was about 13 kb. At any time the percentage of the actively dividing cells was 8.2% of all PBMC. The average TRF length for infants decreases with the maximum rate of about 330 bp/year and this maximum rate corresponds to the age of 1.5 years. Then this rate decreases gradually with time and the rate of shortening of TRF length for adult patients was several folds lower (about 50 bp/year for the age >20–23 years). These estimates of telomere shortening rate with age were close to the values calculated previously (Hastie et al., 1990; Slagboon et al., 1994; van Lunzen et al., 1993; Zeichner et al., 1999) and smaller than the values for the first years of life reported for cross-sectional samples (Frenk et al., 1998; Rufer et al., 1999). The intersection of asymptotic lines for adults and children suggest that at the age of about 6–7 years the rate of telomere length shortening is sharply changed.

Recent advances in inhibition of telomerase activity (Zhang et al., 1999; Hahn et al., 1999; Herbert et al., 1999; Norton et al., 1996; Shammas et al., 1999; Wright et al., 1996) provided a quantitative basis for development of mathematical models. For an in vivo system of low or absent telomerase activity in PBMC, the model presented in this paper describes the telomere dynamics by using parameters that are biologically reasonable: the proportion of actively dividing cells (about 8%) and their half-life ($\ln 2/\hat{q} \sim 20$ days) are in agreement with recent experimental data (Lempicki et al., 2000). It is also in agreement with the results shown in that the rapidly proliferating pool accounts for $\sim$1–10% of proliferating populations of both CD4 and CD8 cells (Kovacs et al., 2001).

The results presented suggest that the rapid telomere shortening in infants is determined by the rapid cell turnover. These results could have implications for elucidation of pathogenesis of pediatric HIV. The rapid turnover of cells susceptible to HIV infection can cause the faster progression of the HIV disease in infants compared to adults.

Acknowledgements

This work was supported, in part, by the National Cancer Institute Short Term Exchange Program to I.S.

References

Allsopp, R.C., Vaziri, H., Patterson, C., Goldstein, S., Younglai, E.V., Futcher, A.B., Greider, C.W., Harley, C.B., 1992. Telomere length predicts replicative capacity of human fibroblasts. Proc. Natl Acad. Sci. USA. 82, 10114–10118.

Blackburn, E.H., 1991. Structure and function of telomeres. Nature 350, 569–573.

Feng, Y.R., Biggar, R.J., Gee, D., Norwood, D., Zeichner, S.L., Dimitrov, D.S., 1999. Long-term telomere dynamics: modest increase of cell turnover in HIV-infected individuals followed for up to 14 years. Pathobiology 67, 34–38.

Frenk, R.W., Blackburn, E.H., Shannon, K.M., 1998. The rate of telomere sequence loss in human leukocytes varies with age. Proc. Natl Acad. Sci. USA. 95, 5607–5610.

Greider, C.W., 1996. Telomere length regulation. Biochemistry 65, 337–365.

Hahn, W.C., Stewart, S.A., Brooks, M.W., York, S.G., Eaton, E., Kurachi, A., Beijersbergen, R.L., Knoll, J.H.M., Meyerson, M., Weinberg, R.A., 1999. Inhibition of telomerase limits the growth of human cancer cells. Nature Med. 5, 1164–1170.

Harley, C.B., 1997. Human ageing and telomeres. In: Chadwick, D.J., Gardew, G. (Eds.), Telomere and Telomerase. Wiley, Chichester, pp. 129–144.

Harley, C.B., Futcher, A.B., Greider, C.W., 1990. Telomeres shorten during ageing of human fibroblasts. Nature 345, 458–460.

Hastie, N.D., Dempster, M., Dunlop, M.G., Thompson, A.M., Green, D.K., Allshire, R.C., 1990. Telomere reduction in human colorecal carcinoma and with aging. Nature 346, 866–868.

Herbert, B.-S., Pitts, A.E., Baker, S.I., Hamilton, S.E., Wright, W.E., Shay, J.W., Corey, D.R., 1999. Inhibition of human telomerase in immortal human cells leads to progressive telomere shortening and cell death. Proc. Natl Acad. Sci. USA. 96, 14281–14286.

Kovacs, J.A., Lempicki, R.A., Sidorov, I.A., Adelsberger, J.W., Herpin, B., Metcalf, J.A., Sereti, I., Polis, M.A., Davey, R.T., Tavel, J., Falloon, J., Stevens, R., Lambert, L., Dewar, R., Schwartzentruber, D.J., Anver, M.R., Baseler, M.W., Masur, H., Dimitrov, D.S., Lane, H.C., 2001. Identification of dynamically distinct subpopulations of T lymphocytes that are differentially affected by HIV. J. Exp. Med. 194, 1731–1741.

Lempicki, R.A., Kovacs, J.A., Baseler, M.W., Adelsberger, J.W., Dewar, L.R., Natarajan, V., Bosche, M.C., Metcalf, J.A., Stevens, R.A., Lambert, L.A., Alvord, W.G., Polis, M.A., Davey, R.T., Dimitrov, D.S., Lane, H.C., 2000. Impact of HIV-1 infection and highly active antiretroviral therapy on the kinetics of CD4+ and CD8+ T cell turnover in HIV-infected patients. Proc. Natl Acad. Sci. USA. 97, 13778–13783.

Marchuk, G.I., Romanyukha, A.A., Bocharov, G.A., 1991. Mathematical model of antiviral immune response. II. Parameter identification for acute viral hepatitis B. J. Theor. Biol. 151, 41–70.

Norton, J.C., Piatyszek, M.A., Wright, W.E., Shay, J.W., Corey, D.R., 1996. Inhibition of human telomerase activity by peptide nucleic acids. Nature Biotechnol. 14, 615–619.

Rufer, N., Brummendorf, T.H., Kolvraa, S., Bischoff, C., Christensen, K., Wadsworth, L., Schulzer, M., Lansdorp, P.M., 1999. Telomere fluorescence measurements in granulocytes and T lymphocyte subsets points to high turnover of hematopoetic stem cells and memory T cells in early childhood. J. Exp. Med. 190, 157–167.

Shammas, M.A., Simmons, C.G., Corey, D.R., Shmookler Reis, R.J., 1999. Telomerase inhibition by peptide nucleic acids revers 'immortality' of transformed human cells. Oncogene 18, 6191–6200.

Sidorov, I.A., Hirsh, K.S., Harley, C.B., Dimitrov, D.S., 2002. Cancer cell dynamics in presence of telomerase inhibitors: analysis of in vitro data. J. Theor. Biol. 219, 225–233.

Sidorov, I.A., Hirsh, K.S., Harley, C.B., Dimitrov, D.S., 2003. Cancer treatment by telomerase inhibitors: predictions by a kinetic model. Math. Biosci. 181, 209–221.

Slagboon, P.E., Droog, S., Boomsma, D.I., 1994. Genetic determination of telomere size in humans: a twin study of three age groups. Am. J. Hum. Genet. 55, 876–881.

Swan, G.W., 1987. Tumor growth models and cancer chemotherapy. In: Thompson, J.R., Brown, B.W. (Eds.), Cancer Modeling. Marcel Dekker, Inc., New York and Basel, pp. 91–179.

Ulaner, G.A., Giudice, L.C., 1997. Developmental regulation of telomerase activity in human fetal tissue during gestation. Mol. Hum. Reproduction 3, 760–773.

van Lunzen, J., Schachter, F., Uchida, I., Wei, L., Zhu, X., Effros, R., Cohen, D., Harley, C.B., 1993. Loss of telomeric DNA during aging of normal and trisomy 21 human lymphocytes. Am. J. Hum. Genet. 52, 661–668.

Weng, N., Levine, B.L., June, C.H., Hodes, R.J., 1995. Human naive and memory T lymphocytes differ in telomeric length and replicative potential. Proc. Natl Acad. Sci. USA. 92, 11091–11094.

Wilson, C., Lewis, D., Penix, L., 1996. The physiologic immunodeficiency of immaturity. In: Stiehm, E. (Ed.), Immunologic Disorders in Infants and Children. Saunders, Philadelphia, PA, pp. 253–278.

Wright, W.E., Piatyszek, M.A., Rainey, W.E., Byrd, W., Shay, J.W., 1996. Telomerase activity in human germline and embryonic tissues and cells. Dev. Genet. 18, 173–179.

Zeichner, S.L., Palumbo, P., Feng, Y., Xiao, X., Gee, D., Sleasman, J., Goodenow, M., Biggar, R., Dimitrov, D., 1999. Rapid telomere shortening in children. Blood 93, 2824–2830.

Zhang, X., Mar, V., Zhou, W., Harrington, L., Robinson, M.O., 1999. Telomere shortening and apoptosis in telomerase-inhibited human tumor cells. Genes Dev. 13, 2388–2399.